Fracture of polymer networks with diverse topological defects

Shaoting Lin[1] and Xuanhe Zhao[1,2,*]

[1]*Department of Mechanical Engineering, Massachusetts Institute of Technology, Cambridge, Massachusetts 02139, USA*
[2]*Department of Civil and Environmental Engineering, Massachusetts Institute of Technology, Cambridge, Massachusetts 02139, USA*

Polymer networks are pervasive in biological organisms and engineering materials. Topological defects such as cyclic loops and dangling chains are ubiquitous in polymer networks. While fracture is a dominant mechanism for mechanical failures of polymer networks, existing models for fracture of polymer networks neglect the presence of topological defects. Here, we report a defect-network fracture model that accounts for the impact of various types of topological defects on fracture of polymer networks. We show that the fracture energy of polymer networks should account for the energy from multiple layers of polymer chains adjacent to the crack. We further show that the presence of topological defects tends to toughen a polymer network by increasing the effective chain length, yet to weaken the polymer network by introducing inactive polymer chains. Such competing effects can either increase or decrease the overall intrinsic fracture energy of the polymer network, depending on the types and densities of topological defects. Our model provides theoretical explanations for the experimental data on the intrinsic fracture energy of polymer networks with various types and densities of topological defects.

I. INTRODUCTION

Polymer networks are pervasive in biological organisms such as extracellular matrices [1] and engineering materials such as elastomers [2] and gels [3,4]. Fracture of polymer networks is a dominant cause of their mechanical failures. Intrinsic fracture energy, the energy required to propagate a crack in a material by a unit area without bulk dissipation, plays a central role in characterizing fracture of polymer networks [5–7]. The current understanding on the intrinsic fracture energy of polymer networks is based on the Lake-Thomas model [8], which accounts for the energy required to fracture a single layer of polymer chains in a polymer network without any topological defect; nevertheless, topological defects such as cyclic loops and dangling chains are ubiquitous in polymer networks. Recent experiments have shown that the Lake-Thomas model underestimates the intrinsic fracture energy of nearly defect-free polymer networks by a few times [9,10]. In addition, as the density of dangling chains in a polymer network increases, the intrinsic fracture energy of the polymer network decreases at a rate slower than its shear modulus decreases. These intriguing yet unexplained experimental results clearly indicate the limitation of the current understanding on fracture of polymer networks.

Burgeoning interests are being focused on understanding the relationship between network structure and fracture behavior [11,12]. For example, through the combined experimental and numerical efforts, Yamaguchi *et al.* [11] studied the critical roles of chain length heterogeneity and functionality heterogeneity in the fracture energy of networks. By developing an adaptive quasicontinuum approach, Elbanna *et al.* [13] investigated the effects of local topology and dis-

order on the network fracture characteristics. Despite these efforts, the impact of various types of topological defects on fracture of polymer networks remains illusive.

Here, we report a defect-network fracture model capable of predicting the intrinsic fracture energy of polymer networks without defect and polymer networks containing various types topological defects including cyclic loops and dangling chains (Fig. 1). We show that the Lake-Thomas model underestimates the intrinsic fracture energy of defect-free polymer networks due to the negligence of energy stored in the polymer chains adjacent to the fractured chains. The defect-network fracture model is inspired by the recently
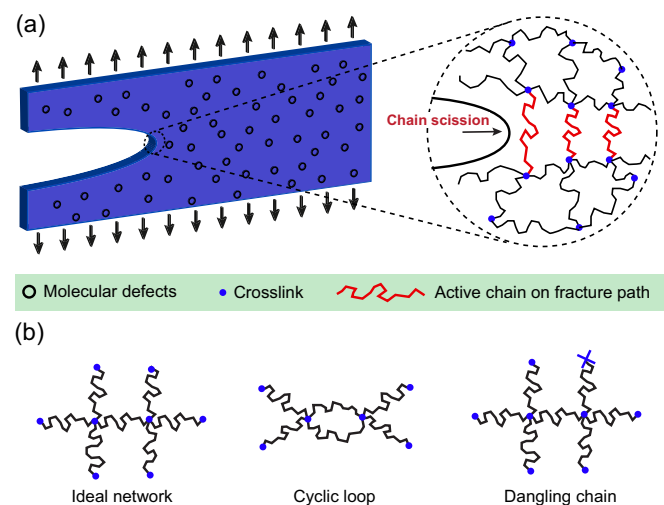

FIG. 1. (a) Schematic illustration of crack propagation in a polymer network with topological defects by fracturing active polymer chains. (b) Cyclic loops and dangling chains are the two most representative types of topological defects in polymer networks.
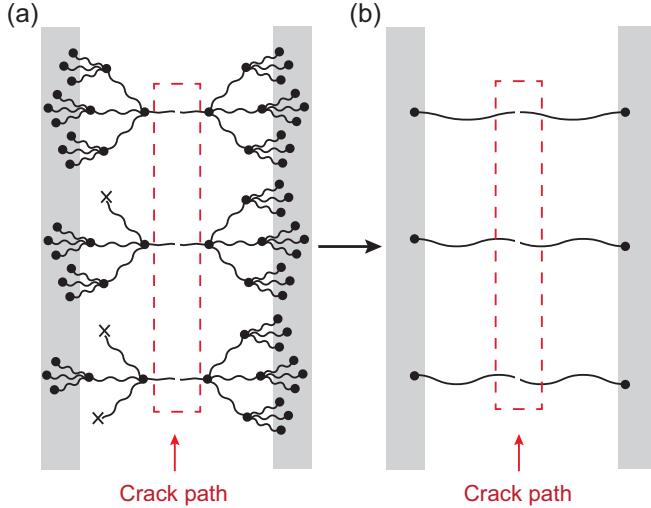
*zhaox@mit.edu

(a) (b)

FIG. 2. Schematic illustration of the defect-network fracture model. (a) Crack propagation in a polymer network with topological defects. (b) The defect-network fracture model gives the same density of fractured polymer chains as that in (a) but effectively longer fractured chain than those in (a). Overall, the defect-network fracture model accounts for the energy in multiple layers of polymer chains adjacent to the fractured chains.

developed real elastic network model [14] or more generally the phantom network model [15,16]. Analogous to the previous models, our model introduces effectively longer fractured chains to account for the energy of the fractured chains (Fig. 2). However, physically different from the previous models, the effectively longer chains in our model do not change the density of the layer of fractured chains (Fig. 2). Overall, our model predicts that the intrinsic fracture energy of defect-free polymer networks is a few times higher than the Lake-Thomas model's prediction. Our model further shows that the presence of topological defects tends to toughen a polymer network by increasing the effective chain length, yet to weaken the polymer network by introducing inactive polymer chains. Such competing effects can either increase or decrease the overall intrinsic fracture energy of the polymer network, depending on the types and densities of topological defects introduced. For example, the introduction of second-order loops [Fig. 1(b)] into a polymer network increases its intrinsic fracture energy but decreases its shear modulus; the presence of first-, second-, third-, or fourth-order dangling chains [Fig. 1(b)] in a polymer network decreases its intrinsic fracture energy at rates slower than the reduction rates of its shear modulus. Furthermore, our model explains the experimental data on the intrinsic fracture energy of nearly defect-free polymer networks and polymer networks with varying densities of first-, second-, third-, or fourth-order dangling chains [9].

II. FRACTURE OF DEFECT-FREE IDEAL POLYMER NETWORKS

Without loss of generality, let us consider an ideal polymer network that has uniform chain length and no defect. The functionality of the polymer network f denotes the number

of polymer chains at each cross-linking point. Note f should be equal to or greater than 3 for polymer networks. The propagation of a crack in the ideal polymer network will fracture a layer of polymer chains on the crack path [8]. While the elasticity of a polymer chain depends on its entropy, the fracture of the polymer chain is energetic [Figs. 3(a) and 3(b)]. Recent experiments [17,18] and simulations [19,20] have shown that the force-extension relations for the energetic elongation and fracture of polymer chains are approximately linear and that the entropic effect on the fracture energy of polymer chains is negligible [for example, Fig. 3(a) [17,18,21,22]. Given these observations, we approximate the fracture energy of the polymer chain as that of a linear elastic spring by $U_{\text{chain}} = F_f^2/(2S)$, where F_f is the force required to fracture the chain and S is the spring constant of the fully extended chain [20,23]. The crack propagation will relax the energy stored in the fractured polymer chains as well as the adjacent polymer chains. In a real sample, the structure of a tetra-arm polymer network is a three-dimensional tetrahedron lattice, similar to the topology of a diamond [24]. Here, we focus on the simplified two-dimensional lattice structure for the calculation, which has been well adopted by the classical affine and phantom network models in polymer elasticity [15,16] and the classical Lake-Thomas model in polymer fracture [8]. As illustrated in Fig. 3(c), the fracture force F_f of a polymer chain on the crack path (denoted as $i = 0$) is equally shared by the $f - 1$ neighboring chains on each of its two ends (denoted as $i = -1$ or $+1$). The force in a chain with $i = -1$ or $+1$ is further equally shared by the neighboring chains on its left or right side (denoted as $i = -2$ or $+2$), respectively. In this way, the maximum force in the ith polymer chains can be calculated as $F_f/(f - 1)^{|i|}$. Based on the linear-chain assumption, the total energy stored in and relaxed by all ith polymer chains can be calculated as $U_i = U_{\text{chain}}/(f - 1)^{|i|}$, which is plotted in Fig. 3(d). Overall, the effective energy relaxed by fracturing a polymer chain in the ideal polymer network can be calculated as

$$U_{\text{ideal}} = \sum_{-\infty}^{\infty} U_i = \frac{f}{f - 2} U_{\text{chain}}. \quad (1)$$

In comparison, the energy relaxed by fracturing a polymer chain in the Lake-Thomas model is only U_0 or U_{chain}. Since the energy required to fracture a polymer chain is linearly proportional to the chain length [8], the polymer chains adjacent to the fractured chains in our model give effectively longer fractured chains compared with the Lake-Thomas model, while not changing the area density of the fractured chains (Fig. 2). Therefore, our model predicts that the intrinsic fracture energy of ideal polymer networks is $f/(f - 2)$ times the value given by the Lake-Thomas model. The effect of the neighboring chains on the intrinsic fracture energy can be significant, especially for ideal polymer networks with low functionality f [Fig. 3(e)]. For example, for a tetra-arm ideal network (i.e., $f = 4$), the intrinsic fracture energy predicted by our model is two times the value predicted by the Lake-Thomas model, implying that the fracture energy of ideal polymer networks without defects should account for the energy from multiple layers of polymer chains. Notably, recent experiments have indeed shown that the Lake-Thomas model underestimates
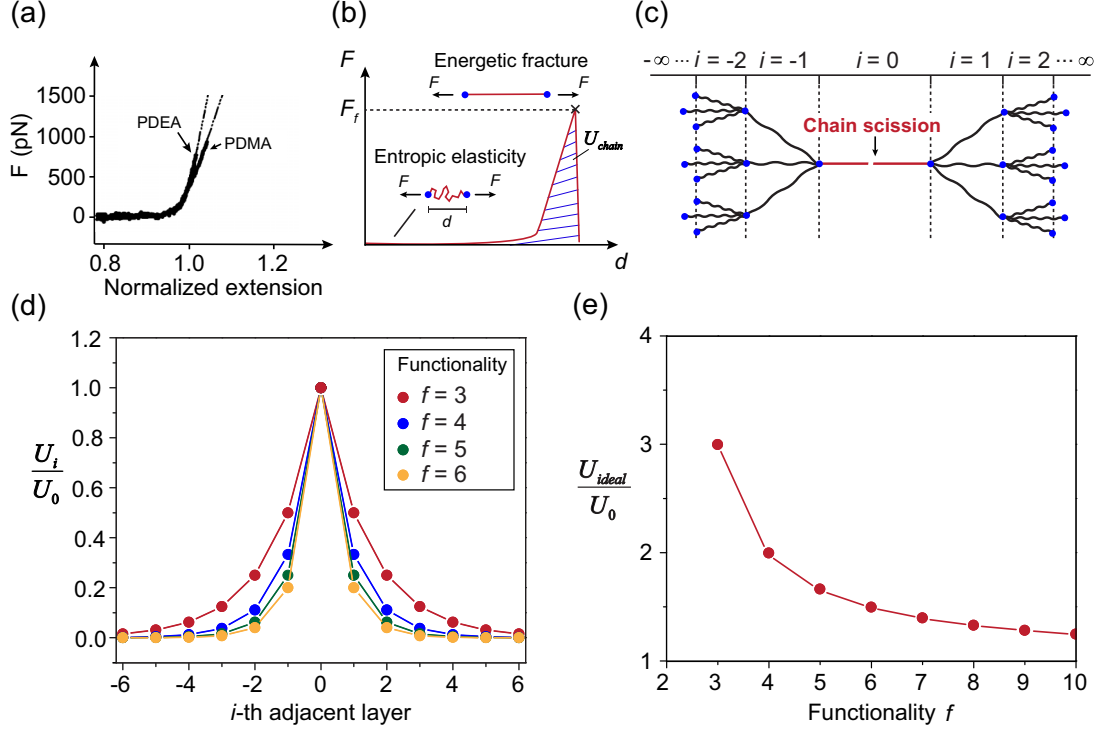
FIG. 3. (a) Experimentally measured force-extension curves of two single polymer chains [i.e., poly(N, N'-dimethylacrylamide) (PDMA) and poly(N, N'-diethylacrylamide) (PDEA)] by force spectroscopy [17]. (b) Schematic illustration of the force-extension curve of a single polymer chain, the enclosed area of which defines the fracture energy of the chain U_{chain}. (c) Schematic illustration of a fractured polymer chain on the crack path (i.e., $i = 0$) and deformed neighboring chains (i.e., $|i| > 0$). (d) The energy relaxed by all ith polymer chains U_i normalized by the fracture energy of an ideal chain on the crack path U_0 in ideal polymer networks with functionality $f = 3$, 4, 5, and 6. (e) The effective energy relaxed by fracturing a polymer chain in the ideal polymer network U_{ideal} normalized by the fracture energy of the chain on the crack path U_0 as a function of the functionality f.

the measured intrinsic fracture energy of nearly defect-free tetra-arm networks by around three times [9].

III. FRACTURE OF POLYMER NETWORKS WITH TOPOLOGICAL DEFECTS

Next, we will present a defect-network fracture model to predict the intrinsic fracture energy of polymer networks containing various cyclic loops [14,25] and dangling chains [26,27]—two of the most representative types of topological defects. Because existing experiments are based on tetra-arm networks with uniform chain length [9], we focus on tetra-arm networks with topological defects in this paper ($f = 4$). The introduction of a cyclic loop or a dangling chain into an ideal polymer network can affect its intrinsic fracture energy by changing the energy required to fracture polymer chains affected by the defect and/or by introducing inactive polymer chains. Let us denote the energy required to fracture a polymer chain that is most affected by a defect X as U_X; let us further define the fracture effectiveness of this polymer chain as $\gamma_X = U_X/U_{ideal}$, where U_{ideal} is the effective energy by fracturing an unaffected ideal chain in the same network. We next calculate the U_X and γ_X for various topological defects in a tetra-arm network. Notably, it is reasonable to assume that the defects in the polymer network are sparsely distributed and thus do not interact with one another [14,25,27,28].

When the defect is a second-order loop, denoted as $X = 2l$, the most affected polymer chains are the chains in the loop itself. As illustrated in Fig. 4(a), the fracture force $2F_f$ of a second-order loop on the crack path (denoted as $i = 0$) is equally shared by the two neighboring chains on each of its two ends (denoted as $i = -1$ or $+1$). The force in a chain with $i = -1$ or $+1$ is further shared by the three neighboring chains on its left or right side (denoted as $i = -2$ or $+2$), respectively. In this way, the maximum force sustained by each ith polymer chain can be calculated as $F_f/3^{|i|-1}$ with its relaxed energy as $U_{chain}/3^{2|i|-2}$ for $|i| \geqslant 1$. Since the number of ith polymer chains for $|i| \geqslant 1$ is $2 \times 3^{|i|-1}$, the total energy relaxed by all ith polymer chains can be calculated as $U_i = 2U_{chain}/3^{|i|-1}$ for $|i| \geqslant 1$ and $U_i = 2U_{chain}$ for $i = 0$ [Fig. 4(b)]. Overall, the effective energy relaxed by fracturing a second-order loop on the crack path is equal to $\sum_{-\infty}^{\infty} U_i = 8U_{chain}$. Since there are two chains in a second-order loop, based on the aforementioned definition, we can get $U_{2l} = \sum_{-\infty}^{\infty} U_i/2 = 4U_{chain}$ and $\gamma_{2l} = U_{2l}/U_{ideal} = 2$. Notably, the fracture effectiveness of polymer chains other than the most affected chains by a second-order loop is approximately 1 (as shown in Supplemental Material Figs. S1 and S5 [29]), and thus we regard these chains as unaffected chains to simplify the calculation. In addition, both theory and simulations have indicated that the densities of higher-order loops are negligibly low in tetra-arm networks [26]; therefore, we mainly focus on the second-order loops in the current study.
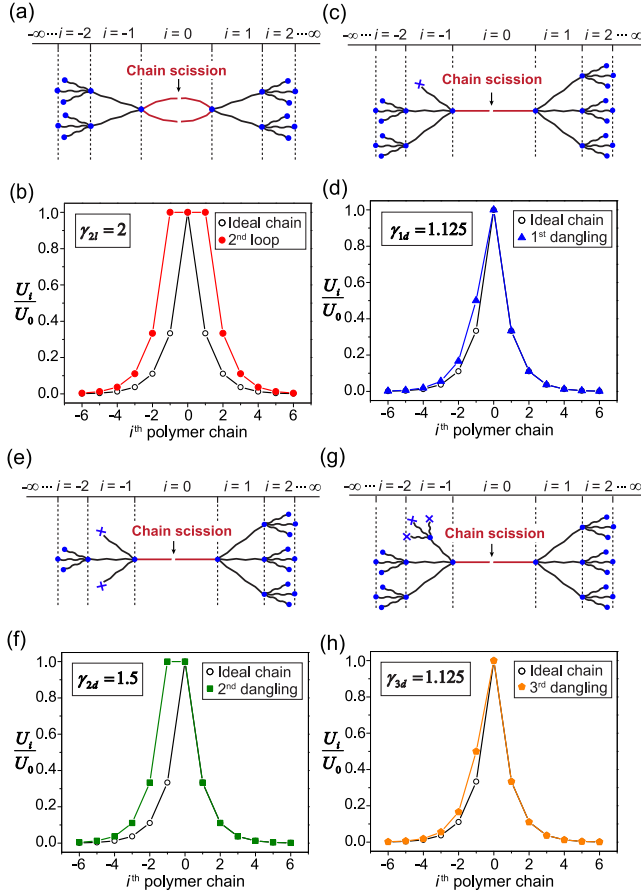
FIG. 4. (a) Schematic illustration of a fractured second-order loop on the crack path and deformed neighboring chains. (b) The energy relaxed by all ith polymer chains U_i normalized by the fracture energy of a second-order loop on the crack path U_0, compared with that of an ideal chain. (c) Schematic illustration of a fractured chain closest to a first-order dangling chain and deformed neighboring chains. (d) The energy relaxed by all ith polymer chains U_i normalized by the fracture energy of the most affected chain by a first-order dangling chain on the crack path U_0, compared with that of an ideal chain. (e) Schematic illustration of a fractured chain closest to a second-order dangling chain and deformed neighboring chains. (f) The energy relaxed by all ith polymer chains U_i normalized by the fracture energy of the most affected chain by a second-order dangling chain on the crack path U_0, compared with that of an ideal chain. (g) Schematic illustration of a fractured chain closest to a third-order dangling chain and deformed neighboring chains. (h) The energy relaxed by all ith polymer chains U_i normalized by the fracture energy of the most affected chain by a third-order dangling chain on the crack path U_0, compared with that of an ideal chain.

When the defect is a first-order dangling chain, denoted as $X = 1d$, the most affected polymer chain is the closest neighbor of the defect as illustrated in Fig. 4(c). The fracture force F_f of the most affected chain on the crack path (denoted as $i = 0$) is shared by two neighboring chains at one end of the chain (denoted as $i = -1$) and by three neighboring chains at the other end of the chain (denoted as $i = +1$). The force in each of the ith polymer chains is further shared by three neighboring $(i-1)$th or $(i+1)$th chains. The total energy stored in

the ith polymer chains can be calculated as $U_i = U_{\text{chain}}$ for $i = 0$, $U_i = U_{\text{chain}}/(2 \times 3^{|i|-1})$ for $i \leqslant -1$, and $U_i = U_{\text{chain}}/3^{|i|}$ for $i \geqslant 1$ [Fig. 4(d)]. Overall, the effective energy relaxed by fracturing the closest chain to the first-order dangling chain can be calculated as $U_{1d} = \sum_{-\infty}^{\infty} U_i = 2.25 U_{\text{chain}}$, with its fracture effectiveness equal to $\gamma_{1d} = U_{1d}/U_{\text{ideal}} = 1.125$. When the defect is a second-order dangling chain, denoted as $X = 2d$, the most affected polymer chain is the closest neighbor of the defect as illustrated in Fig. 4(e). The total energy stored in the ith polymer chains can be calculated as $U_i = U_{\text{chain}}$ for $i = -1, 0$, $U_i = U_{\text{chain}}/3^{|i|}$ for $i \geqslant 1$, and $U_i = U_{\text{chain}}/3^{|i|-1}$ for $i \leqslant -2$ [Fig. 4(f)]. Overall, the effective energy relaxed by fracturing the closest chain to a second-order dangling chain can be calculated as $U_{2d} = \sum_{-\infty}^{\infty} U_i = 3 U_{\text{chain}}$ with its fracture effectiveness equal to $\gamma_{2d} = U_{2d}/U_{\text{ideal}} = 1.5$. When the defect is a third-order dangling chain, denoted as $X = 3d$, the defect turns its closest neighbor into a first-order dangling chain and the most affected polymer chain is the closest neighbor of the effectively first-order dangling chain as illustrated in Fig. 4(g). The total energy stored in and relaxed by all ith polymer chains is the same as that for a first-order dangling chain [Fig. 4(h)]. Overall, the effective energy relaxed by fracturing the most affected chain by the third-order dangling chain can be calculated as $U_{3d} = \sum_{-\infty}^{\infty} U_i = 2.25 U_{\text{chain}}$ with its fracture effectiveness equal to $\gamma_{3d} = U_{3d}/U_{\text{ideal}} = 1.125$. When the defect is a fourth-order dangling chain, denoted as $X = 4d$, the defect affects no polymer chains in the tetra-arm network. In addition, the fracture effectiveness of polymer chains other than the most affected chains by the dangling chains is approximately 1 (as shown in Supplemental Material Figs. S2– S5 [29]), and thus we regard these chains as unaffected chains to simplify the calculation.

The introduction of defects into an ideal polymer network not only alters the fracture effectiveness of the most affected chains, but also reduces the density of active chains. The tetra-arm network is composed of tetra-arm macromers [24]; therefore, a defect X in the tetra-arm network is introduced by the corresponding macromer(s) with the defect X. Let C_X and C_{ideal} be the ratios of the numbers of macromers with defect X and defect-free macromers over the total number of macromers that constitute the polymer network, respectively. The number conservation of macromers imposes $\sum_X C_X + C_{\text{ideal}} = 1$. Once cross-linked, the macromers form the polymer network with defects. We denote N_X^{inactive} and N_X^{affected} as the number of inactive chains and the most affected chains due to the presence of defect X, respectively, and $N^{\text{unaffected}}$ as the number of unaffected chains. The number conservation of polymer chains imposes $\sum_X (N_X^{\text{affected}} + N_X^{\text{inactive}}) + N^{\text{unaffected}} = N$, where N is the total number of polymer chains in the corresponding defect-free ideal network. Next, we will calculate the N_X^{affected} and N_X^{inactive} corresponding to each type of macromer with defect X in the tetra-arm network.

For a tetra-arm network containing only the second-order loops, there exist no inactive polymer chains $N_{2l}^{\text{inactive}} = 0$. Among the active chains, the number of affected chains by the second-order loops is equal to $N_{2l}^{\text{affected}} = (C_{2l}/2)N$, since half of the arms of defect macromers are associated with the second-order loops. For a tetra-arm network containing only the first-order dangling chains, the number of inactive chains is equal to $N_{1d}^{\text{inactive}} = (C_{1d}/4)N$, since one-fourth of the arms
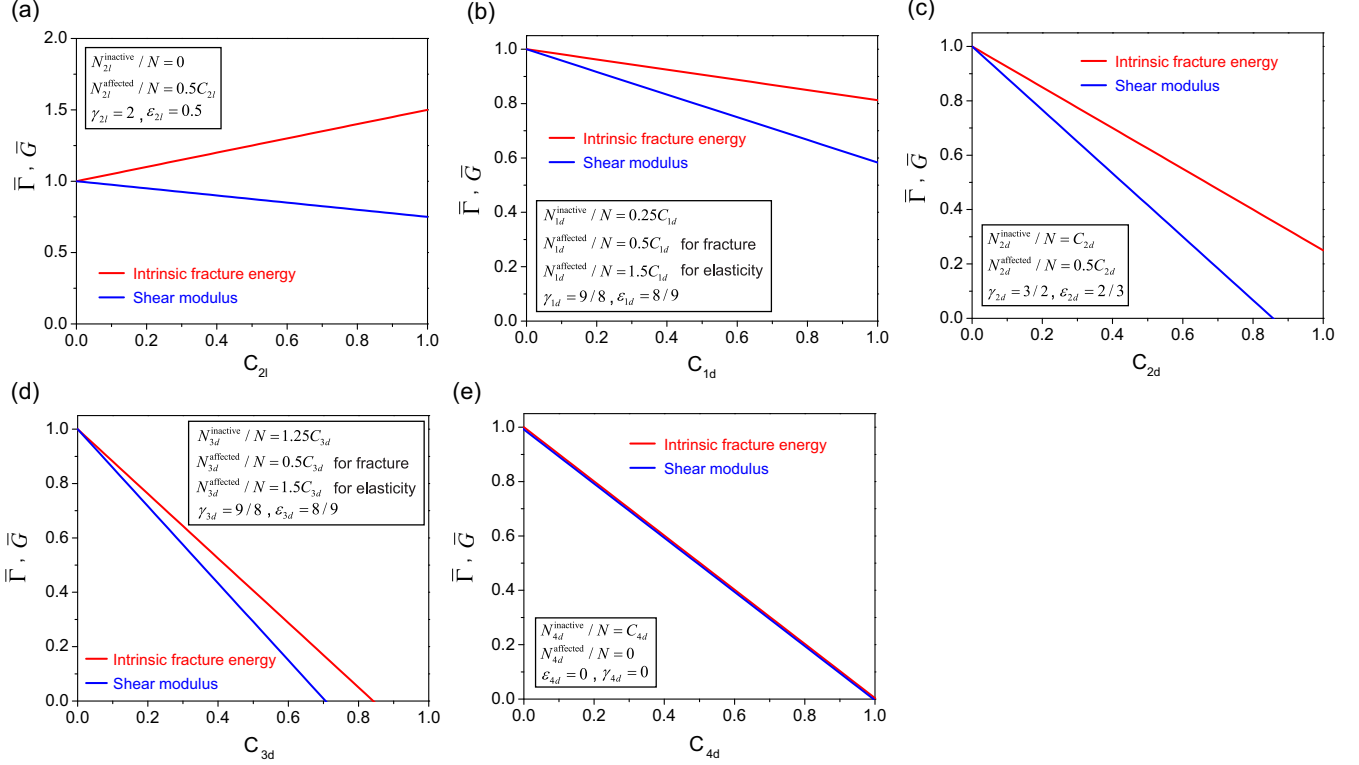
FIG. 5. Normalized intrinsic fracture energy and normalized shear modulus of polymer networks containing only one type of topological defect. (a) Second-order loop with $\gamma_{2l} = 2$ and $\varepsilon_{2l} = \frac{1}{2}$. (b) First-order dangling with $\gamma_{1d} = \frac{9}{8}$ and $\varepsilon_{1d} = \frac{8}{9}$. (c) Second-order dangling with $\gamma_{2d} = \frac{3}{2}$ and $\varepsilon_{2d} = \frac{2}{3}$. (d) Third-order dangling with $\gamma_{2d} = \frac{9}{8}$ and $\varepsilon_{2d} = \frac{8}{9}$. (e) Fourth-order dangling with $\gamma_{2d} = 0$ and $\varepsilon_{2d} = 0$. The intrinsic fracture energy and shear modulus are normalized by the corresponding values of defect-free polymer networks.

of defect macromers are inactive arms. The number of the most affected chains due to the presence of the first-order dangling chains is equal to $N_{1d}^{\text{affected}} = (C_{1d}/2)N$, since two defect macromers possess one affected chain. For a tetra-arm network containing only the second-order dangling chains, the introduction of defect macromers only increases the length of originally existing chains. In other words, all arms of defect macromers are inactive arms, giving the number of inactive chains as $N_{2d}^{\text{inactive}} = (C_{2d})N$. The number of affected chains due to the presence of the second-order dangling chains are $N_{2d}^{\text{affected}} = (C_{2d}/2)N$, since two defect macromers possess one affected chain. For a polymer network containing only the third-order dangling chains, the presence of a macromer with three inactive arms leads to one more inactive chain from the neighboring macromer. Therefore, we can calculate the numbers of inactive chains and affected chains due to the presence of the third-order dangling chains as $N_{3d}^{\text{inactive}} = (5C_{3d}/4)N$ and $N_{3d}^{\text{affected}} = (C_{3d}/2)N$, respectively. For a polymer network containing only the fourth-order dangling chains, the defect macromers have no topological connection with the polymer network, thereby possessing no affected chains, namely, $N_{4d}^{\text{affected}} = 0$. The introduced number of inactive chains is $N_{4d}^{\text{inactive}} = C_{4d}N$. The densities of inactive chains and affected chains in polymer networks containing one specific type of defect are summarized in Table I.

Overall, the intrinsic fracture energy of the polymer network with defects normalized by that of the corresponding defect-free ideal network can be expressed as $\overline{\Gamma} = \sum_X \gamma_X (N_X^{\text{affected}}/N) + (N^{\text{unaffected}}/N)$. Given $N^{\text{unaffected}} = N - $

$\sum_X (N_X^{\text{affected}} + N_X^{\text{inactive}})$, we can further express the normalized intrinsic fracture energy of polymer networks with defects as

$$\overline{\Gamma} = \sum_X (\gamma_X - 1)\frac{N_X^{\text{affected}}}{N} - \sum_X \frac{N_X^{\text{inactive}}}{N} + 1, \qquad (2)$$

where the first term $(\gamma_X - 1)N_X^{\text{affected}}/N$ increases the intrinsic fracture energy of the polymer network by increasing the fracture effectiveness of the most affected chains (i.e., $\gamma_X \geqslant 1$), and the second term $-\sum_X N_X^{\text{inactive}}/N$ decreases the intrinsic fracture energy of the polymer network by introducing inactive chains.

We further derive a defect-network elastic model to calculate the shear modulus of polymer networks with topological defects by calculating the elastic effectiveness of the most affected chains ε_X [14,26] and the densities of affected chains N_X^{affected} and inactive chains N_X^{inactive} when the defect X is introduced (Supplemental Material). Overall, the shear modulus of polymer networks with various defects normalized by that of the corresponding defect-free ideal network can be expressed as

$$\overline{G} = \sum_X (\varepsilon_X - 1)\frac{N_X^{\text{affected}}}{N} - \sum_X \frac{N_X^{\text{inactive}}}{N} + 1, \qquad (3)$$

where the first term $(\varepsilon_X - 1)N_X^{\text{affected}}/N$ decreases the shear modulus of the polymer network since $\varepsilon_X < 1$, and the second

TABLE I. Normalized numbers of inactive chains, unaffected chains, and affected chains, as well as the fracture effectiveness and elastic effectiveness of affected chains in defect-network fracture and elastic models for tetra-arm polymer networks containing various types of topological defects.

	Defect-network fracture model				Defect-network elastic model			
	$N^{\text{unaffected}}/N$	N_X^{inactive}/N	N_X^{affected}/N	γ_X	$N^{\text{unaffected}}/N$	N_X^{inactive}/N	N_X^{affected}/N	ε_X
Second-order loop	$1 - 0.5C_{2l}$	0	$0.5C_{2l}$	2	$1 - 0.5C_{2l}$	0	$0.5C_{2l}$	0.5
First-order dangling	$1 - 0.75C_{1d}$	$0.25C_{1d}$	$0.5C_{1d}$	9/8	$1 - 1.75C_{1d}$	$0.25C_{1d}$	$1.5C_{1d}$	8/9
Second-order dangling	$1 - 1.5C_{2d}$	C_{2d}	$0.5C_{2d}$	3/2	$1 - 1.5C_{2d}$	C_{2d}	$0.5C_{2d}$	2/3
Third-order dangling	$1 - 1.75C_{3d}$	$1.25C_{3d}$	$0.5C_{3d}$	9/8	$1 - 2.75C_{3d}$	$1.25C_{3d}$	$1.5C_{3d}$	8/9
Fourth-order dangling	$1 - C_{4d}$	C_{4d}	0	0	$1 - C_{4d}$	C_{4d}	0	0

term $-\sum_X N_X^{\text{inactive}}/N$ also decreases the shear modulus of the polymer network by introducing inactive chains.

Table I summarizes the normalized numbers of inactive chains, unaffected chains, and affected chains as well as the fracture effectiveness and elastic effectiveness of affected chains. We also systematically compare the impact of topological defects on fracture energy and elasticity of the same polymer networks as summarized in Fig. 5 and Table I. In Fig. 5, we plot the $\overline{\Gamma}$ and $\overline{G}$ of tetra-arm networks containing each type of topological defect as functions of the corresponding C_X. It can be seen that the presence of second-order loops in the polymer network increases its intrinsic fracture energy but decreases its shear modulus. In addition, when dangling chains are introduced, although both the instrinsic fracture energy and shear modulus decrease, the reduction of the intrinsic fracture energy is less dramatic.

IV. EXPLANATION OF EXPERIMENTAL DATA

Next, we will use our defect-network fracture model to explain the reported experimental data on the intrinsic fracture energy of tetra-arm polymer networks with varying densities of first-, second-, third-, or fourth-order dangling chains [9]. The amounts of various orders of dangling chains can be readily tuned by controlling the reaction efficiency p between two arms that form a polymer chain. The formation of various orders of loops is negligible according to the experiments,

theory, and simulations [9,26]. Applying the Miller-Mascoko theory [30,31], we calculate $C_{1d} = 4(1 - P)^3 P$, $C_{2d} = 6(1 - P)^2 P^2$, $C_{3d} = 4(1 - P)P^3$, and $C_{4d} = P^4$, where $P = pP^3 + 1 - p$ is the probability of forming a dangling chain for one of the arms in a tetra-arm macromer [31] [Fig. 6(a)]. Following the relations between C_X, N_X^{inactive}, and N_X^{affected}, and using Eq. (2), we can calculate the normalized intrinsic fracture energy of the tetra-arm network $\overline{\Gamma}$ as a function of the reaction efficiency p,

$$\overline{\Gamma} = 1 - \frac{3}{4}(1 - P)^3 P - \frac{9}{2}(1 - P)^2 P^2 - \frac{19}{4}(1 - P)P^3 - P^4.$$

(4)

In addition, with N_X^{inactive} and N_X^{affected}, and Eq. (3), we calculate the normalized shear modulus of the tetra-arm network $\overline{G}$ as a function of the reaction efficiency p (see details in the Supplemental Material),

$$\overline{G} = 1 - \frac{5}{3}(1 - P)^3 P - 7(1 - P)^2 P^2 - \frac{17}{3}(1 - P)P^3 - P^4.$$

(5)

One intriguing yet unexplained discovery from the experiments [9] is that as the reaction efficiency p decreases (i.e., as the defect density increases) the intrinsic fracture energy of the polymer network decreases at a rate slower than the shear modulus decreases [Fig. 6(b)]. Our model can readily explain this phenomenon. While the dangling chains introduce the
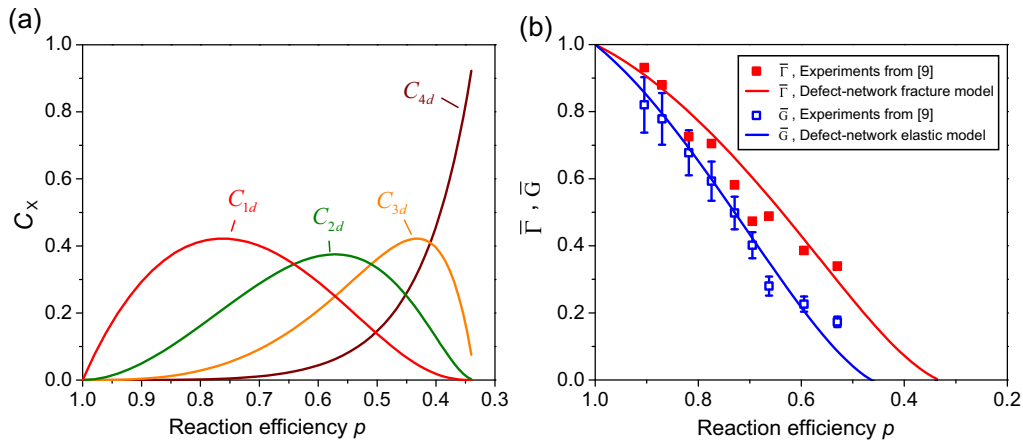

FIG. 6. (a) Ratios of the numbers of macromers with various orders of dangling chains over the total number of macromers that constitute the tetra-arm polymer network (i.e., C_{1d}, C_{2d}, C_{3d}, and C_{4d}) as functions of the reaction efficiency p. (b) Comparison of the normalized intrinsic fracture energy and the normalized shear modulus between the experiment results [9] and the defect-network models.

same amount of inactive polymer chains (i.e., N_X^{inactive}) for both fracture and elasticity of the polymer network, they increase the fracture effectiveness [i.e., $\gamma_X \geqslant 1$ in Eq. (2)] of the most affected chains but decrease the elastic effectiveness [i.e., $\varepsilon_X < 1$ in Eq. (3)] of the most affected chains. Therefore, the intrinsic fracture energy reduces slower than the shear modulus does with the increase of the defect density. As plotted in Fig. 6(b), our defect-network models also match well with the experimental data [9] on the intrinsic fracture energy $\overline{\Gamma}$ and shear modulus $\overline{G}$ of the tetra-arm network across a wide range of reaction efficiency and densities of various dangling chains.

V. SUMMARY AND DISCUSSION

We have developed a defect-network fracture model that characterizes the impact of topological defects on the intrinsic fracture energy of polymer networks. Based on the model, we explain the experimental results [9] on the intrinsic fracture energy of nearly defect-free polymer networks and polymer networks with varying densities of first-, second-, third-, or fourth-order dangling chains. We show that the fracture energy of polymer networks should account for the energy from multiple layers of polymer chains adjacent to the crack. Our model further suggests that, although the presence of topological defects inevitably decreases the shear moduli of polymer networks, it can enhance the intrinsic fracture energy considerably by introducing second-order loops while suppressing dangling chains—a theoretical prediction that can be validated by future experiments. With the recent development in engineering [32,33] and characterizing[34–36] topological defects in polymer networks, our model opens an avenue to establishing a relationship between fracture energy of polymer networks and their topological structures.

[1] L. Casares, R. Vincent, D. Zalvidea, N. Campillo, D. Navajas, M. Arroyo, and X. Trepat, Hydraulic fracture during epithelial stretching, Nat. Mater. **14**, 343 (2015).

[2] E. Ducrot, Y. Chen, M. Bulters, R. P. Sijbesma, and C. Creton, Toughening elastomers with sacrificial bonds and watching them break, Science **344**, 186 (2014).

[3] J.-Y. Sun, X. Zhao, W. R. Illeperuma, O. Chaudhuri, K. H. Oh, D. J. Mooney, J. J. Vlassak, and Z. Suo, Highly stretchable and tough hydrogels, Nature (London) **489**, 133 (2012).

[4] J. P. Gong, Y. Katsuyama, T. Kurokawa, and Y. Osada, Double-network hydrogels with extremely high mechanical strength, Adv. Mater. **15**, 1155 (2003).

[5] S. Lin, X. Liu, J. Liu, H. Yuk, H.-C. Loh, G. A. Parada, C. Settens, J. Song, A. Masic, G. H. McKinley *et al.*, Anti-fatigue-fracture hydrogels, Sci. Adv. **5**, eaau8528 (2019).

[6] S. Lin, J. Liu, X. Liu, and X. Zhao, Muscle-like fatigue-resistant hydrogels by mechanical training, Proc. Natl. Acad. Sci. USA **116**, 10244 (2019).

[7] R. Bai, Q. Yang, J. Tang, X. P. Morelle, J. Vlassak, and Z. Suo, Fatigue fracture of tough hydrogels, Extreme Mech. Lett. **15**, 91 (2017).

[8] G. Lake and A. Thomas, The strength of highly elastic materials, Proc. R. Soc. A **300**, 108 (1967).

[9] Y. Akagi, H. Sakurai, J. P. Gong, U.-i. Chung, and T. Sakai, Fracture energy of polymer gels with controlled network structures, J. Chem. Phys. **139**, 144905 (2013).

[10] R. Long, C.-Y. Hui, J. P. Gong, and E. Bouchbinder, The fracture of highly deformable soft materials: A tale of two length scales, Ann. Rev. Condens. Matter Phys. (to be published), arXiv:2004.03159.

[11] T. Yamaguchi, Y. Onoue, and Y. Sawae, Topology and Toughening of Sparse Elastic Networks, Phys. Rev. Lett. **124**, 068002 (2020).

[12] K. Kothari, Y. Hu, S. Gupta, and A. Elbanna, Mechanical response of two-dimensional polymer networks: role of topology, rate dependence, and damage accumulation, J. Appl. Mech. **85**, 031008 (2018).

[13] A. Ghareeb and A. Elbanna, An adaptive quasicontinuum approach for modeling fracture in networked materials: Application to modeling of polymer networks, J. Mech. Phys. Solids **137**, 103819 (2020).

[14] M. Zhong, R. Wang, K. Kawamoto, B. D. Olsen, and J. A. Johnson, Quantifying the impact of molecular defects on polymer network elasticity, Science **353**, 1264 (2016).

[15] M. Rubinstein, R. H. Colby *et al.*, *Polymer Physics* (Oxford University Press, New York, 2003), Vol. 23.

[16] H. M. James and E. Guth, Theory of the Elastic Properties of Rubber, J. Chem. Phys. **11**, 455 (1943).

[17] C. Wang, W. Shi, W. Zhang, X. Zhang, Y. Katsumoto, and Y. Ozaki, Force spectroscopy study on poly (acrylamide) derivatives: Effects of substitutes and buffers on single-chain elasticity, Nano Lett. **2**, 1169 (2002).

[18] K. Wang, X. Pang, and S. Cui, Inherent stretching elasticity of a single polymer chain with a carbon–carbon backbone, Langmuir **29**, 4315 (2013).

[19] W. Wang, K. A. Kistler, K. Sadeghipour, and G. Baran, Molecular dynamics simulation of afm studies of a single polymer chain, Phys. Lett. A **372**, 7007 (2008).

[20] Y. Mao, B. Talamini, and L. Anand, Rupture of polymers by chain scission, Extreme Mech. Lett. **13**, 17 (2017).

[21] C. Ortiz and G. Hadziioannou, Entropic elasticity of single polymer chains of poly (methacrylic acid) measured by atomic force microscopy, Macromolecules **32**, 780 (1999).

[22] S. Yamamoto, Y. Tsujii, and T. Fukuda, Atomic force microscopic study of stretching a single polymer chain in a polymer brush, Macromolecules **33**, 5995 (2000).

[23] S. Wang, S. Panyukov, M. Rubinstein, and S. L. Craig, Quantitative adjustment to the molecular energy parameter in the

lakethomas theory of polymer fracture energy, Macromolecules **52**, 2772 (2019).

[24] T. Sakai, T. Matsunaga, Y. Yamamoto, C. Ito, R. Yoshida, S. Suzuki, N. Sasaki, M. Shibayama, and U.-i. Chung, Design and fabrication of a high-strength hydrogel with ideally homogeneous network structure from tetrahedron-like macromonomers, Macromolecules **41**, 5379 (2008).

[25] R. Wang, A. Alexander-Katz, J. A. Johnson, and B. D. Olsen, Universal Cyclic Topology in Polymer Networks, Phys. Rev. Lett. **116**, 188302 (2016).

[26] T.-S. Lin, R. Wang, J. A. Johnson, and B. D. Olsen, Topological structure of networks formed from symmetric four-arm precursors, Macromolecules **51**, 1224 (2018).

[27] Y. Gu, J. Zhao, and J. A. Johnson, A (macro) molecular-level understanding of polymer network topology, Trends Chem. **1**, 318 (2019).

[28] R. Wang, J. A. Johnson, and B. D. Olsen, Odd–even effect of junction functionality on the topology and elasticity of polymer networks, Macromolecules **50**, 2556 (2017).

[29] See Supplemental Material at http://link.aps.org/supplemental/10.1103/PhysRevE.102.052503 for details about the effects of topological distance of fractured chains from topological defects.

[30] C. W. Macosko and D. R. Miller, A new derivation of average molecular weights of nonlinear polymers, Macromolecules **9**, 199 (1976).

[31] Y. Akagi, T. Matsunaga, M. Shibayama, U.-i. Chung, and T. Sakai, Evaluation of topological defects in tetra-peg gels, Macromolecules **43**, 488 (2010).

[32] H. Zhou, J. Woo, A. M. Cok, M. Wang, B. D. Olsen, and J. A. Johnson, Counting primary loops in polymer gels, Proc. Natl. Acad. Sci. USA **109**, 19119 (2012).

[33] K. Kawamoto, M. Zhong, R. Wang, B. D. Olsen, and J. A. Johnson, Loops versus branch functionality in model click hydrogels, Macromolecules **48**, 8980 (2015).

[34] Y. Chen, C. J. Yeh, Y. Qi, R. Long, and C. Creton, From force-responsive molecules to quantifying and mapping stresses in soft materials, Sci. Adv. **6**, eaaz5093 (2020).

[35] J. M. Clough, C. Creton, S. L. Craig, and R. P. Sijbesma, Covalent bond scission in the Mullins effect of a filled elastomer: Real-time visualization with mechanoluminescence, Adv. Funct. Mater. **26**, 9063 (2016).

[36] J. Slootman, V. Waltz, C. J. Yeh, C. Baumann, R. Göst, J. Comtet, and C. Creton, Quantifying and mapping covalent bond scission during elastomer fracture, arXiv:2006.09468 (2020).

Supplementary Information for

Fracture of polymer networks with diverse topological defects

Shaoting Lin[1], Xuanhe Zhao[1,2]

[1]Department of Mechanical Engineering, Massachusetts Institute of Technology, Cambridge, MA 02139, USA

[2]Department of Civil and Environmental Engineering, Massachusetts Institute of Technology, Cambridge, MA 02139, USA

1. Effects of topological distance of fractured chains from topological defects

In the model, we regard polymer chains other than the most affected chains as unaffected ideal chains to simply the calculation. To validate this assumption, we systematically calculate the fracture effectiveness of polymer chains as a function of the topological distance m of fractured polymer chains from different types of topological defects.

We start with a polymer network containing 2nd-order loops. When topological distance m is equal to 1 [**Fig. S1(b)**], the 2nd-order loop is located at the 1st adjacent layer attach to the fractured polymer chain on the crack path, at which each of the chains shares the maximum mechanical force on the order of $F_c / 3$ and contributes to the bond energy on the order of $U_0 / 9$. The total energy stored at the 1st adjacent layer containing 2nd-order loops is on the order of $U_0 / 3$, i.e., $U_{-1} = U_0 / 3$, which is the same as that attached to an ideal chain. The 2nd adjacent layer contains 5 polymer chains in total, among which 3 active chains share the maximum mechanical force on the order of $F_c / 9$ with the total energy on the order of $U_0 / 27$ and the other 2 active chains share the maximum mechanical force on the order of $F_c / 3$ with the total energy on the order of $2U_0 / 9$. The total energy stored at the 2nd adjacent layer containing 2nd-order loops is on the order of $7U_0 / 27$, i.e., $U_{-2} = 7U_0 / 27$. The energy stored at the other end of adjacent layers shows the same energy distributions as that attached to an ideal chain due to the same topological structures. In summary, the normalized energy distributions around crack path when $m = 1$ can be expressed as

2

$$
\frac{U_i}{U_0} =
\begin{cases}
\dfrac{7}{27 \cdot 3^{|i|-2}} & i \leq -2 \\[2mm]
\dfrac{1}{3} & i = -1 \\[2mm]
1 & i = 0 \\[2mm]
\dfrac{1}{3^{|i|}} & i \geq 1
\end{cases}
\tag{S1}
$$

Similarly, we can derive the normalized energies contributed by the adjacent layers when $m = 2$ [**Fig. S1(c)**] expressed as

$$
\frac{U_i}{U_0} =
\begin{cases}
\dfrac{13}{243 \cdot 3^{|i|-3}} & i \leq -3 \\[2mm]
\dfrac{1}{3^{|i|}} & -2 \leq i \leq -1 \\[2mm]
1 & i = 0 \\[2mm]
\dfrac{1}{3^{|i|}} & i \geq 1
\end{cases}
\tag{S2}
$$

The expression of the normalized energies contributed by the adjacent layers reads as

$$
\frac{U_i}{U_0} =
\begin{cases}
\dfrac{3^m + 4}{3^{2m+1} \cdot 3^{|i|-m-1}} & i \leq -m-1 \\[2mm]
\dfrac{1}{3^{|i|}} & -m \leq i \leq -1 \\[2mm]
1 & i = 0 \\[2mm]
\dfrac{1}{3^{|i|}} & i \geq 1
\end{cases}
\tag{S3}
$$

For polymer networks containing 1st-order dangling chains, when the topological distance is equal to 1 [**Fig. S2(b)**], the 1st-order dangling chain is located at the 1st layer adjacent to the primary polymer chain at the crack path, at which each of the chains shares the maximum mechanical force on the order of $F_c/3$ and contributes to the energy on the order of $U_0/9$. The total energy stored

3

at the 1st adjacent layer containing 1st-order dangling chains is on the order of $U_0/3$, i.e.,

$U_{-1} = U_0/3$. The 2nd layer adjacent contains 8 active chains in total, among which 6 chains share

the maximum mechanical force on the order of $F_c/9$ with the total energy on the order of $2U_0/27$

and the other 2 chains share the maximum mechanical force on the order of $F_c/6$ with the total

energy on the order of $U_0/18$. The total energy stored at the 2nd adjacent layer containing 1st-order

loops is on the order of $7U_0/54$, i.e., $U_{-2} = 7U_0/54$. In summary, the normalized energy

distributions around crack path when $m=1$ can be expressed as

$$\frac{U_i}{U_0} = \begin{cases} \dfrac{7}{54 \cdot 3^{|i|-2}} & i \le -2 \\ \dfrac{1}{3} & i = -1 \\ 1 & i = 0 \\ \dfrac{1}{3^{|i|}} & i \ge 1 \end{cases} \tag{S4}$$

Similarly, we can derive the normalized energies contributed by the adjacent layers when $m=2$

[**Fig. S2(c))**] expressed as

$$\frac{U_i}{U_0} = \begin{cases} \dfrac{19}{486 \cdot 3^{|i|-3}} & i \le -3 \\ \dfrac{1}{3^{|i|}} & -2 \le i \le -1 \\ 1 & i = 0 \\ \dfrac{1}{3^{|i|}} & i \ge 1 \end{cases} \tag{S5}$$

The expression of the normalized energy distributions for the scission of the chain with the

topological distance of *m* away from 1st-order dangling chains is

4

$$\frac{U_i}{U_0} = \begin{cases} \dfrac{2\cdot 3^m + 1}{2\cdot 3^{2m+1}\cdot 3^{|i|-m-1}} & i \le -m-1 \\[3mm] \dfrac{1}{3^{|i|}} & -m \le i \le -1 \\[3mm] 1 & i = 0 \\[3mm] \dfrac{1}{3^{|i|}} & i \ge 1 \end{cases} \tag{S6}$$

For polymer networks containing 2nd-order dangling chains, when the topological distance is equal to 1 [**Fig. S3(b)**], the 2nd-order dangling chain is located at the 1st layer adjacent to the primary polymer chain at the crack path, at which each of the chains shares the maximum mechanical force on the order of $F_c/3$ and contributes to the bond energy on the order of $U_0/9$. In total, the energy stored at the 1st adjacent layer containing 2nd-order dangling chains is on the order of $U_0/3$, i.e., $U_{-1} = U_0/3$. The 2nd layer adjacent contains 7 polymer chains in total, among which 6 chains share the maximum mechanical force on the order of $F_c/9$ with the total energy on the order of $2U_0/27$ and the other 1 chain share the maximum mechanical force on the order of $F_c/3$ with the bond energy on the order of $U_0/9$. The total energy stored at the 2nd adjacent layer containing 2nd-order dangling loops is on the order of $6U_0/27$, i.e., $U_{-2} = 6U_0/27$. In summary, the normalized energy distributions around crack path when $m=1$ can be expressed as

$$\frac{U_i}{U_0} = \begin{cases} \dfrac{6}{27\cdot 3^{|i|-2}} & i \le -2 \\[3mm] \dfrac{1}{3} & i = -1 \\[3mm] 1 & i = 0 \\[3mm] \dfrac{1}{3^{|i|}} & i \ge 1 \end{cases} \tag{S7}$$

5

Similarly, we can derive the normalized energies contributed by the adjacent layers when $m = 2$ [**Fig. S3(c)**] expressed as

$$\frac{U_i}{U_0} = \begin{cases} \dfrac{11}{243 \cdot 3^{|i|-3}} & i \leq -3 \\[2mm] \dfrac{1}{3^{|i|}} & -2 \leq i \leq -1 \\[2mm] 1 & i = 0 \\[2mm] \dfrac{1}{3^{|i|}} & i \geq 1 \end{cases} \tag{S8}$$

The expression of the normalized energy distributions for the scission of the chain with the topological distance of m away from 2nd-order dangling chains is

$$\frac{U_i}{U_0} = \begin{cases} \dfrac{3^m + 2}{3^{2m+1} \cdot 3^{|i|-m-1}} & i \leq -m-1 \\[2mm] \dfrac{1}{3^{|i|}} & -m \leq i \leq -1 \\[2mm] 1 & i = 0 \\[2mm] \dfrac{1}{3^{|i|}} & i \geq 1 \end{cases} \tag{S9}$$

For polymer networks containing 3rd-order dangling chains, when the topological distance is equal to 1 [**Fig. S4(b)**], the 3rd-order dangling chain is located at the 1st layer adjacent to the primary polymer chain at the crack path, at which each of the chains shares the maximum mechanical force on the order of $F_c / 3$ and contributes to the bond energy on the order of $U_0 / 9$. The total energy stored at the 1st adjacent layer containing secondary loops is on the order of $U_0 / 3$, i.e., $U_{-1} = U_0 / 3$, which is the same as that of ideal chains. The 2nd layer adjacent contains 8 polymer chains in total, among which 6 chains share the maximum mechanical force on the order of $F_c / 9$ with the bond energy in total on the order of $2U_0 / 27$ and the other 2 chains share the maximum

6

mechanical force on the order of $F_c/6$ with the total energy on the order of $U_0/18$. The total energy stored at the 2nd adjacent layer containing 3rd-order is on the order of $7U_0/54$, i.e., $U_{-2} = 7U_0/54$. In summary, the normalized energy distributions around crack path when $m=1$ can be expressed as

$$\frac{U_i}{U_0} = \begin{cases} \dfrac{7}{54 \cdot 3^{|i|-2}} & i \leq -2 \\ \dfrac{1}{3} & i = -1 \\ 1 & i = 0 \\ \dfrac{1}{3^{|i|}} & i \geq 1 \end{cases} \qquad (S10)$$

Similarly, we can derive the normalized energies contributed by the adjacent layers when when $m=2$ [**Fig. S4(c)**] as

$$\frac{U_i}{U_0} = \begin{cases} \dfrac{19}{486 \cdot 3^{|i|-3}} & i \leq -3 \\ \dfrac{1}{3^{|i|}} & -2 \leq i \leq -1 \\ 1 & i = 0 \\ \dfrac{1}{3^{|i|}} & i \geq 1 \end{cases} \qquad (S11)$$

The expression of the normalized energy distributions for the scission of the chain with the topological distance of m away from 3rd-order dangling chains is

7

$$\frac{U_i}{U_0} = \begin{cases} \dfrac{2 \cdot 3^m + 1}{2 \cdot 3^{2m+1} \cdot 3^{|i|-m-1}} & i \le -m-1 \\[3ex] \dfrac{1}{3^{|i|}} & -m \le i \le -1 \\[3ex] 1 & i = 0 \\[3ex] \dfrac{1}{3^{|i|}} & i \ge 1 \end{cases} \tag{S12}$$

Figure S5 summarizes the fracture effectiveness of the affected polymer chains by various topological defects as a function of topological distance m, validating our assumption that the polymer chains other than the most affected chains can be regarded as unaffected ideal chains.

2. Defect-network elastic model

2.1. Elasticity of defect-free ideal polymer networks

We first recall the classical phantom network model to calculate the shear modulus of a defect-free ideal polymer network. Let M_{chain} be the chain length (i.e., the number of monomers in an active chain) in polymer networks and f be the functionality of crosslinkers in the polymer network. Each ideal polymer chain is equally connected to $f-1$ neighboring chains on each of its two ends (denoted as $i = -1$ or $+1$). The force in a chain with $i = -1$ or $+1$ is further equally connected to the neighboring chains on its left or right side (denoted as $i = -2$ or $+2$), respectively. In this way, the effective chain length of all i^{th} polymer chains can be calculated as $M_i = M_{chain} / (f-1)^{|i|}$. Overall, the total effective chain length by elastically deforming an ideal polymer chain can be calculated as

$$M_{ideal} = \sum_{-\infty}^{\infty} M_i = \frac{f}{f-2} M_{chain} \tag{S13}$$

Because of the conservation of monomers, the increase of the chain length from M_{chain} to M_{ideal} in a phantom network leads to a reduced number density of active chains in an equivalent affine polymer network. Let v be the number density of active polymer chains in a phantom polymer network. Its shear modulus is equal to $G_{ideal} / kT = v\left(M_{chain} / M_{ideal}\right) = v\left(f - 2\right) f^{-1}$ with kT being the product of Boltzmann constant and temperature.

2.2. Elasticity of polymer networks with topological defects

Elastic effectiveness of affected chains. Next, we will present a defect-network elastic model to predict the shear modulus of polymer networks with cyclic loops and dangling chains. We focus on tetra-arm networks in this work ($f = 4$). The introduction of a cyclic loop or a dangling chain into an ideal polymer network can affect its shear modulus by changing the effective chain length affected by the defect and/or by introducing inactive polymer chains. We denote the effective chain length for deforming the most affected polymer chain by the defect X as M_X; we further define the elastic effectiveness of this polymer chain is defined as $\varepsilon_X = M_{ideal} / M_X$, where M_{ideal} is the effective chain length of an ideal chain, following the recently developed real elastic network model [1, 2]. We next calculate the M_X and ε_X for various topological defects in a tetra-arm network. The defects in the polymer network are assumed to be sparsely distributed and have no interaction with each other [2].

When the defect is a 2nd-order loop, denoted as $X=2l$, the most affected chains are the chains in the loop itself. As illustrated in **Fig. S6(a)**, the effective chain length of one 2nd-order loop is $M_{chain} / 2$. One 2nd-order loop is equally connected to the 2 neighboring chains on each its ends (denoted as $i = -1$ or $+1$), the effective chain length of which is also equal to $M_{chain} / 2$. Each

9

chain with $i = -1$ or $+1$ is further connected to the 3 neighboring chains on its left or right side (denoted as $i = -2$ or $+2$), respectively. In this way, the effective chain length of all i^{th} polymer chains can be calculated as $M_i = 0.5 M_{chain} / 3^{|i|-1}$ for $|i| \geq 1$ [**Fig. S6(b)**]. Overall, the total effective chain length by deforming a 2nd-order loop is equal to $\sum_{-\infty}^{+\infty} M_i = 2M_{chain}$. Since there are two chains in a 2nd-order loop, based on the aforementioned definition, we can get $M_{2l} = 2\sum_{-\infty}^{+\infty} M_i = 4M_{chain}$ and $\varepsilon_{2l} = M_{ideal} / M_{2l} = 0.5$ where $M_{ideal} = 2M_{chain}$ is the effective chain length by elastically deforming an ideal polymer chain. Notably, according to the previous calculations [2], the elastic effectiveness of polymer chains other than the most affected by a 2nd-order loop is approximately 1, and thus we regard these chains as unaffected chains to simplify the calculation.

When the defect is a 1st-order dangling chain, denoted as $X=1d$, the most affected polymer chain is the closest neighbor of the defect as illustrated in **Fig. S6(c)**. The most affected chain is connected to 2 neighboring chains at one end of the chain (denoted as $i = -1$) and to 3 neighboring chains at the other end of the chain (denoted as $i = +1$). Each ith polymer chain is further equally connected to 3 neighboring $(i-1)^{th}$ chains or $(i+1)^{th}$ chains. The effective chain length of all i^{th} polymer chains can be expressed as $M_i = M_{chain}$ for $i = 0$, $M_i = M_{chain} / (2 \cdot 3^{|i|-1})$ for $i \leq -1$, and $M_i = M_{chain} / 3^{|i|-1}$ for $i \geq 1$ [**Fig. S6(d)**]. Overall, the effective chain length by elastically deforming the closest chain to the 1st-order dangling chain can be calculated as $M_{1d} = \sum_{-\infty}^{+\infty} M_i = 2.25 M_{chain}$ with its elastic effectiveness equal to $\varepsilon_{1d} = M_{ideal} / M_{1d} = 8/9$. When the defect is a 2nd-order dangling chain, denoted as $X=2d$, the most affected polymer chain is the

closet neighbor of the defect as illustrated in **Fig. S6(e)**. The effective chain length of all i^{th} polymer chains can be calculated as $M_i = M_{chain}$ for $i = -1$, 0, $M_i = M_{chain} / 3^{|i|}$ for $i \geq 1$, and $M_i = M_{chain} / 3^{|i|-1}$ for $i \leq -2$ [**Fig. S6(f)**]. Overall, the total effective chain length by elastically deforming the most affected chain by a 2nd-order dangling chain can be calculated as

$$M_{2d} = \sum_{-\infty}^{+\infty} M_i = 3M_{chain}$$ with its elastic effectiveness equal to $\varepsilon_{2d} = M_{ideal} / M_{2d} = 2/3$. When the

defect is a 3rd-order dangling chain, denoted as $X=3d$, the defect turns its closet neighbor into a 1st-order dangling chain and the most affected polymer chain is the closest neighbor of the effectively 1st-order dangling chain as illustrated in **Fig. S6(h)**. Overall, the total effective chain length by elastically deforming the most affected chain by a 3rd-order dangling chain can be calculated as

$$M_{3d} = \sum_{-\infty}^{+\infty} M_i = 2.25M_{chain}$$ with its elastic effectiveness equal to $\varepsilon_{3d} = M_{ideal} / M_{3d} = 8/9$. When

the defect is a 4th-order dangling chain, denoted as $X=4d$, the defect affects no polymer chains in the tetra-arm network. In addition, the fracture effectiveness of polymer chains other than the most affected chains by the dangling chains is approximately 1 [1], and thus we regard these chains as unaffected chains to simplify the calculation.

Numbers of affected and inactive chains. The introduction of topological defects not only affects the elastic effectiveness of affected polymer chains, but also alters the chain densities. We focus on a tetra-arm polymer network, a defect X in which is introduced by the corresponding macromer(s) with the defect X. Let C_X and C_{ideal} be the ratios of the numbers of macromers with defect X and defect-free macromers over the total number of macromers that constitute the polymer network, respectively. The number conservation of macromers impose $\sum_X C_X + C_{ideal} = 1$. Once

crosslinked, the macromers form the polymer network with defects. We denote N_X^{inactive} and

N_X^{affected} as the number of inactive chains and the most affected chains due to the presence of defect

X, respectively. Let $N^{\text{unaffected}}$ be the number of unaffected ideal chains. The number conservation

of polymer chains imposes $\sum_X \left(N_X^{\text{affected}} + N_X^{\text{inactive}} \right) + N^{\text{unaffected}} = N$, where N is the total number of

polymer chains in the corresponding defect-free ideal network. Next, we will calculate the N_X^{inactive}

and N_X^{affected} corresponding to each type of macromers with defect X in the tetra-arm polymer

network.

For a tetra-arm network containing only the 2$^{\text{nd}}$-order loops, there exist no inactive polymer

chains $N_{2l}^{\text{inactive}} = 0$. Among the active chains, the number of affected chains by the 2$^{\text{nd}}$-order loops

is equal to $N_{2l}^{\text{affected}} = \left(C_{2l} / 2 \right) N$, since two of the arms of defect macromers are associated with the

2$^{\text{nd}}$-order loops. For a polymer network containing only the 1$^{\text{st}}$-order dangling chains, the number

of inactive chains is equal to $N_{1d}^{\text{inactive}} = \left(C_{1d} / 4 \right) N$, since one-fourth arms of f-arm defect

macromers are inactive. Unlike the defect-network fracture model, the number of the most affected

chain by 1$^{\text{st}}$-order dangling chains is $N_{1d}^{\text{affected}} = 1.5 C_{1d} N$, since two defect macromers possess all

three affected chains. For a polymer network containing only the 2$^{\text{nd}}$-order dangling chains, all

arms of defect macromers are inactive arms, giving the number of inactive chains as

$N_{2d}^{\text{inactive}} = C_{2d} N$. The number of affected chain chains due to the presence of 2$^{\text{nd}}$-order dangling

chains are $N_{2d}^{\text{affected}} = 0.5 C_{2d} N$, since two defect macromers possess one affected chain. For a

polymer network containing only the 3$^{\text{rd}}$-order dangling chains, the presence of a macromer with

three inactive arms leads to one more inactive chain from the neighboring macromer. Therefore,

we can calculate the numbers of inactive chains and affected chains due to the presence of the 3$^{\text{rd}}$-order dangling chains as $N_{3d}^{\text{inactive}} = (5C_{3d}/4)N$ and $N_{3d}^{\text{affected}} = 1.5C_{3d}N$, respectively. For a polymer network containing only the 4$^{\text{th}}$-order dangling chains, the defect macromers have no topological connection with the polymer network, thereby possessing no affected chains, namely, $N_{4d}^{\text{affected}} = 0$. The introduced number of inactive chains is $N_{4d}^{\text{inactive}} = C_{4d}N$.

Shear modulus. Overall, the shear modulus of a polymer network containing defects normalized by that of the corresponding defect-free ideal network can be expressed as

$$\bar{G} = \sum_X \varepsilon_X \left(N_X^{\text{affected}} / N \right) + N^{\text{unaffected}} / N \ , \quad \text{where} \quad N^{\text{unaffected}} / N = 1 - \sum_X \left(N_X^{\text{affected}} / N + N_X^{\text{inactive}} / N \right).$$

Alternatively, the normalized shear modulus can be expressed as

$$\bar{G} = \sum_X (\varepsilon_X - 1) \frac{N_X^{\text{affected}}}{N} - \sum_X \frac{N_X^{\text{inactive}}}{N} + 1 \tag{S14}$$

where the first term $(\varepsilon_X - 1) N_X^{\text{affected}} / N$ decreases the shear modulus of the polymer network since $\varepsilon_X < 1$, and the second term $-\sum_X N_X^{\text{inactive}} / N$ also decreases the shear modulus of the polymer network by introducing inactive chains.

3. **Calculation of normalized intrinsic fracture energy and shear modulus for tetra-arm polymer networks with various types of dangling chains**

We apply the Miller Mascoko theory [3, 4] to calculate the number density of each type of macromer in hydrogels formed by tetra-arm polymer precursors. To apply the theory, we focus on A-B type tetra-arm hydrogels formed by macromer A and macromer B. We presume that 1) all functional end groups of the same type of macromers are equally reactive and 2) all end groups react independently. Let P be the probability of forming dangling chains for one of the arms in

macromers A and macromers B. Given the reaction efficiency p, we can get $P = pP^3 + 1 - p$. Given identified P, the densities of ideal macromers, 1st-order macromers, 2nd-order macromers, 3rd-order macromers, and 4th-order macromers are equal to $C_{ideal} = (1-P)^4$, $C_{1d} = 4(1-P)^3 P$, $C_{2d} = 6(1-P)^2 P^2$, $C_{3d} = 4(1-P)P^3$, and $C_{4d} = P^4$. Once the chemical crosslinking is initiated, the solution of macromers form polymer networks containing various orders of dangling chains. Based on the aforementioned analysis, in our defect-network fracture model, the number of the most affected chains by 1st-/2nd-/3rd/4th-order dangling chains are equal to $N_{1d}^{\text{affected}} = (0.5C_{1d})N$, $N_{2d}^{\text{affected}} = (0.5C_{2d})N$, $N_{3d}^{\text{affected}} = (0.5C_{3d})N$, $N_{4d}^{\text{affected}} = 0$ respectively. The number of inactive chains is equal to $\sum_X N_X^{\text{inactive}} = (0.25C_{1d} + C_{2d} + 1.25C_{3d} + C_{4d})N$. Using Eq. (2), the normalized fracture energy of a tetra-arm polymer network is equal to

$$
\begin{aligned}
\bar{\Gamma} &= 1 - \frac{3}{16}C_{1d} - \frac{3}{4}C_{2d} - \frac{19}{16}C_{3d} - C_{4d} \\
&= 1 - \frac{3}{4}(1-P)^3 P - \frac{9}{2}(1-P)^2 P^2 - \frac{19}{4}(1-P)P^3 - P^4
\end{aligned}
\tag{S15}
$$

In the defect-network elastic model, the normalized densities of the most affected chains by 1st-/2nd-/3rd/4th-order dangling chains are equal to $N_{1d}^{\text{affected}} = (1.5C_{1d})N$, $N_{2d}^{\text{affected}} = (0.5C_{2d})N$, $N_{3d}^{\text{affected}} = (1.5C_{3d})N$, $N_{4d}^{\text{affected}} = 0$ respectively. The number of inactive chains is equal to $\sum_X N_X^{\text{inactive}} = (0.25C_{1d} + C_{2d} + 1.25C_{3d} + C_{4d})N$. Using Eq. (3), the normalized shear modulus of a tetra-arm polymer network is equal to

$$\bar{G} = 1 - \frac{5}{12} C_{1d} - \frac{7}{6} C_{2d} - \frac{17}{12} C_{3d} - C_{4d}$$

$$= 1 - \frac{5}{3}(1-P)^3 P - 7(1-P)^2 P^2 - \frac{17}{3}(1-P)P^3 - P^4 \qquad \text{(S16)}$$
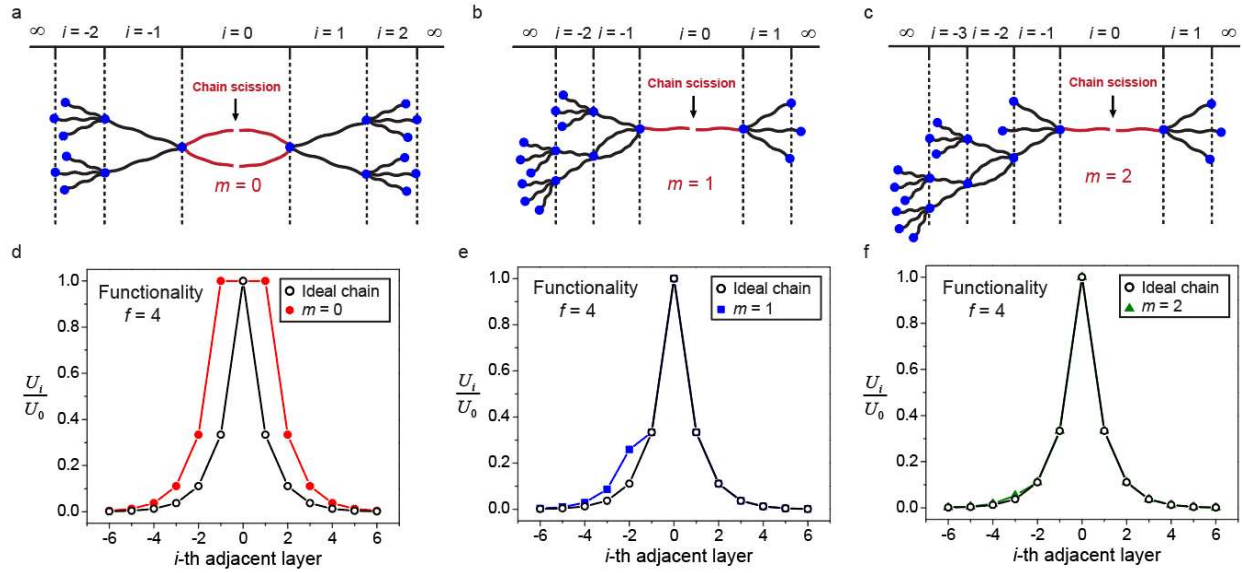
Figure S1. The effect of topological distance of the fractured chain on the crack path from a 2nd-order loop. Schematic illustration of fracturing **a,** the most affected chain by a 2nd-order loop on the crack path (i.e, $m = 0$), **b,** the chain with topological distance of 1 from a 2nd-order loop (i.e, $m = 1$), and **c,** the chain with topological distance of 2 from a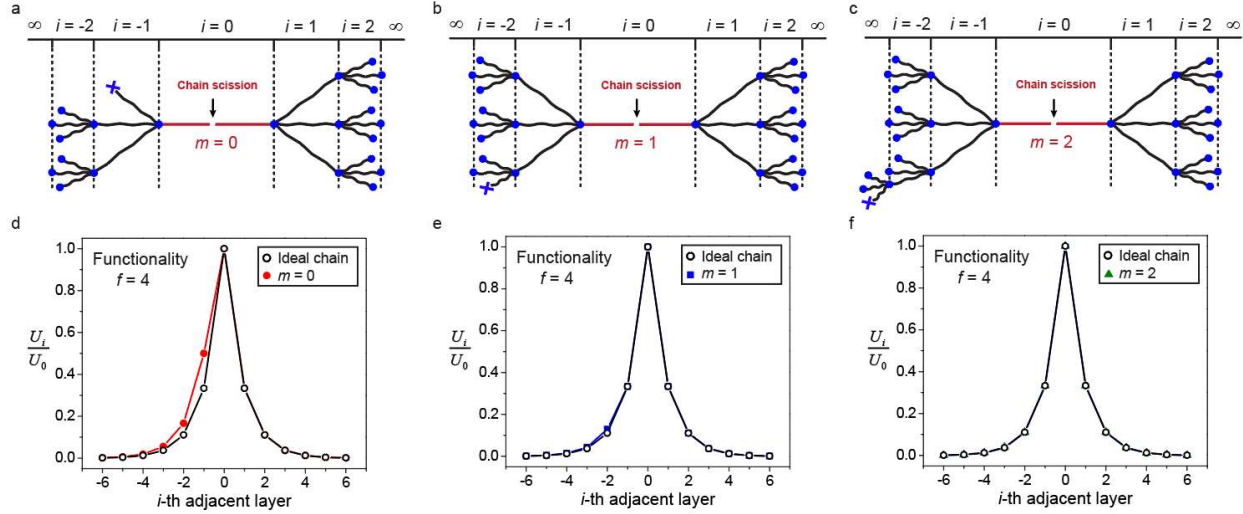 2nd-order loop (i.e, $m = 2$). The normalized energy distributions (i.e., U_i / U_0 versus i^{th} adjacent layer) for fracturing **d,** the most affected chain by a 2nd-order loop in polymer networks (i.e., $m = 0$), **e,** the chain with topological distance of 1 from a 2nd-order loop (i.e, $m = 1$), and **f,** the chain with topological distance of 2 from a 2nd-order loop (i.e, $m = 2$).

Figure S2. The effect of topological distance of fractured chain on the crack path from 1ˢᵗ-order dangling chain. Schematic illustration of fracturing **a,** the most affected chain by 1ˢᵗ-order dangling chain (i.e, $m = 0$), **b**, the chain with topological distance of 1 from 1ˢᵗ-order dangling chain (i.e, $m = 1$), and **c**, the chain with topological distance of 2 from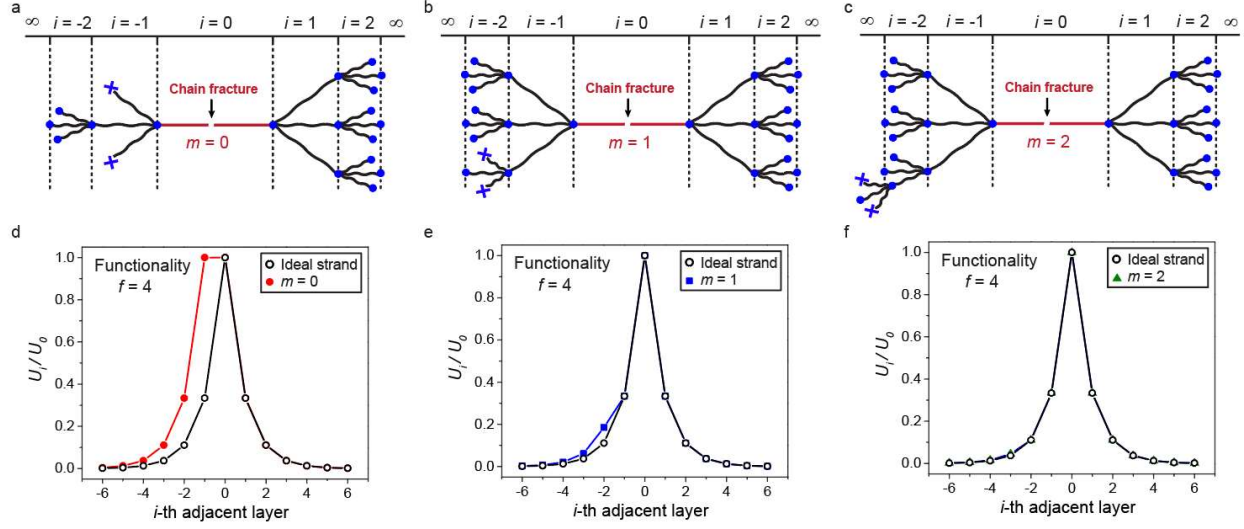 1ˢᵗ-order dangling chain (i.e, $m = 2$). The normalized energy distributions (i.e., U_i / U_0 versus i-th adjacent layer) for fracturing **d**, the most affected chain by 1ˢᵗ-order dangling chain in polymer networks (i.e, $m = 0$), **e**, the chain with topological distance of 1 from 1ˢᵗ-order dangling chain (i.e, $m = 1$), and **f**, the chain with topological distance of 2 from 1ˢᵗ-order dangling chain (i.e, $m = 2$).

Figure S3. The effect of topological distance of fractured chain on the crack path from 2nd-order dangling chain. Schematic illustration of fracuring of **a,** the most affected chain by 2nd-order dangling chain (i.e, $m=0$), **b**, the chain with topological distance of 1 from 2nd-order dangling chain (i.e, $m=1$), and **c**, the chain with topological distance of 2 from 2nd-order dangling chain (i.e, $m=2$). The normalized energy distributions (i.e., U_i/U_0 versus i-th adjacent layer) for fracturing of **d**, the most affected chain by 2nd-order dangling chain in polymer networks (i.e, $m=0$), **e**, the chain with topological distance of 1 from 2nd-order dangling chain (i.e, $m=1$), and **f**, the chain with topological distance of 2 from 2nd-order dangling chain (i.e, $m=2$).
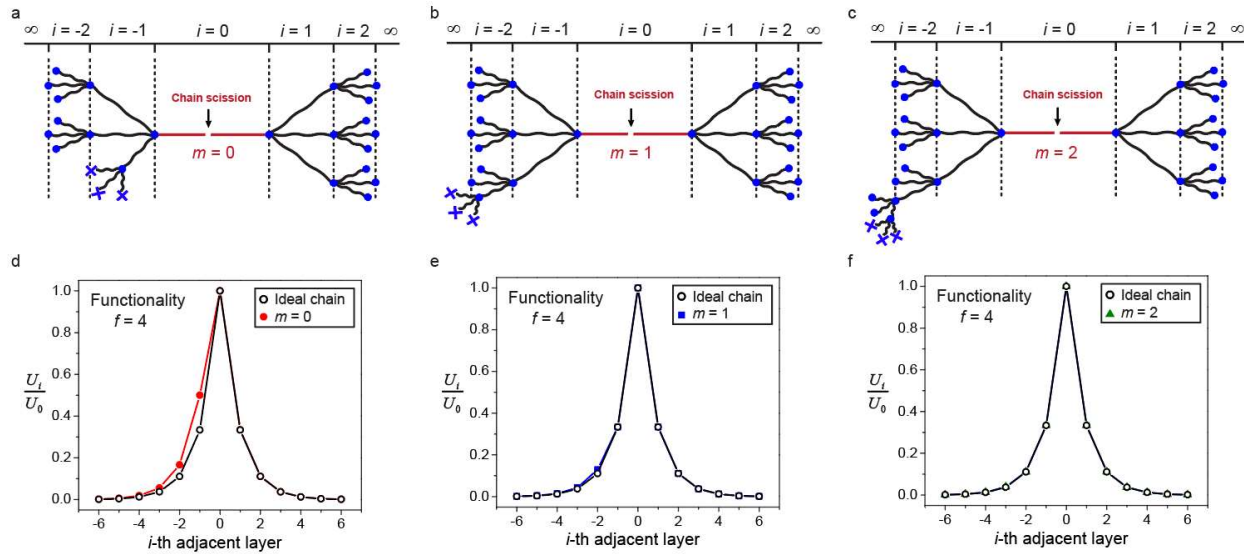
Figure S4. The effect of topological distance of fracturing chain on the crack path from 3rd-order dangling chain. Schematic illustration of the scission of **a,** the most affected chain by 3rd-order dangling chain (i.e, $m=0$), **b**, the chain with topological distance of 1 from 3rd-order dangling chain (i.e, $m=1$), and **c**, the chain with topological distance of 2 from 3rd-order dangling chain (i.e, $m=2$). The normalized energy distributions (i.e., U_i/U_0 versus i-th adjacent layer) for fracturing **d**, the most affected chain by 3rd-order dangling chain in polymer networks (i.e, $m=0$), **e**, the chain with topological distance of 1 from 3rd-order dangling chain (i.e, $m=1$), and **f**, the chain with topological distance of 2 from 3rd-order dangling chain (i.e, $m=2$).
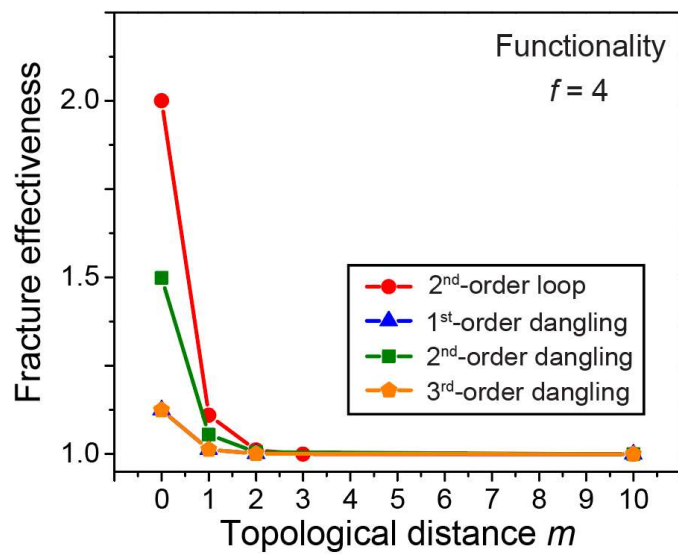
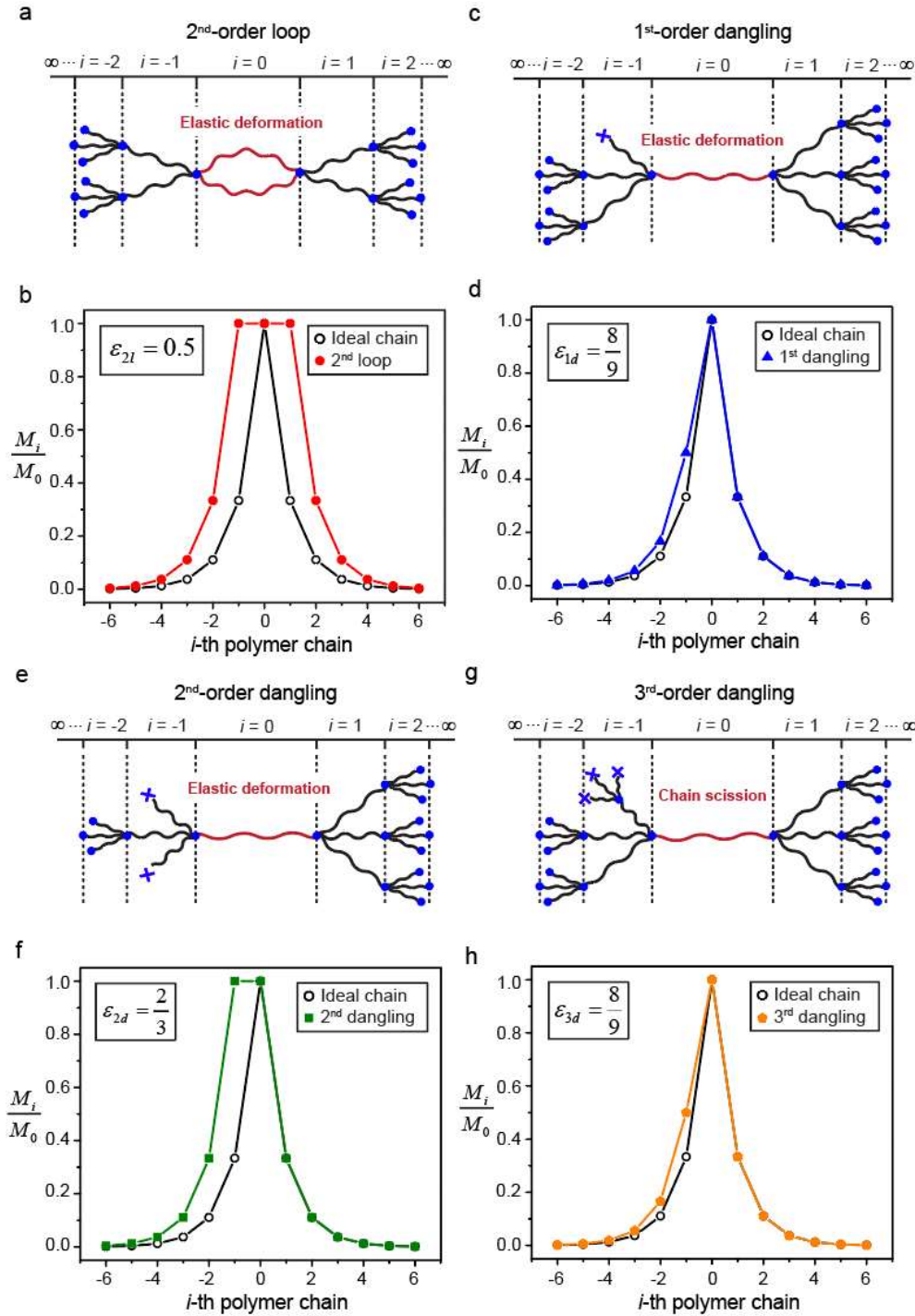**Figure S5. Fracture effectiveness of various topological defects as a function of topological distance *m*.**

Figure S6. a, Schematic illustration of an elastically deformed 2nd-order loop and neighboring chains. **b,** The effective chain length of all i^{th} polymer chains M_i by elastically deforming a 2nd-order loop normalized by the effective chain length of 0th polymer chains M_0. **c,** Schematic illustration of an elastically deformed chain closest to a 1st-order dangling chain and neighboring chains. **d,** The effective chain length of all i^{th} polymer chains M_i by elastically deforming the

closet chain to a 1st-order dangling chain normalized by the chain length of 0th polymer chain M_0. **e,** Schematic illustration of an elastically deformed chain closest to a 2nd-order dangling chain and neighboring chains. **f,** The effective chain length of all i^{th} polymer chains M_i by elastically deforming the closet chain to a 2nd-order dangling chain normalized by the chain length of 0th polymer chain M_0. **g,** Schematic illustration of an elastically deformed chain closest to a 3rd-order dangling chain and neighboring chains. **h,** The effective chain length of all i^{th} polymer chains M_i by elastically deforming the closet chain to a 3rd-order dangling chain normalized by the chain length of 0th polymer chain M_0.

References

1. Lin, T.-S., et al., *Topological structure of networks formed from symmetric four-arm precursors.* Macromolecules, 2018. **51**(3): p. 1224-1231.
2. Zhong, M., et al., *Quantifying the impact of molecular defects on polymer network elasticity.* Science, 2016. **353**(6305): p. 1264-1268.
3. Akagi, Y., et al., *Evaluation of topological defects in tetra-PEG gels.* Macromolecules, 2010. **43**(1): p. 488-493.
4. Macosko, C.W. and D.R. Miller, *A new derivation of average molecular weights of nonlinear polymers.* Macromolecules, 1976. **9**(2): p. 199-206.